Preparation of melanin-silver nanocomposites material and its physiological activity in vitro

Li Gao
North University of China
Lixiao Guo
North University of China
Shuli Zhang
North University of China
Yinghu Zhao (Zhaogao202005@163.com)
North University of China
Jun Xie
Shanxi Medical University
Linlin Liu
North University of China
Hongyu Xu
North University of China

Article

Keywords: Mel-AgNPs, Preparation, Characterization, Physiological activity, Antibacterial

Posted Date: May 17th, 2022

DOI: https://doi.org/10.21203/rs.3.rs-1638328/v1

Abstract

In recent years, due to the potential application of metal nanomaterials in the field of medical sectors, the biological preparation of silver nanoparticles is attracting people's interest. Melanin is a natural biological dye, has a variety of biological functions, and has been widely used in the preparation of composites. In this study, melanin-nanometer silver (Mel-AgNPs) composites were prepared by one-step biological method using silver nitrate as raw material and melanin as reducing agent and coating agent. The ultraviolet - visible spectrum of MEL-AgNPS composites showed the maximum absorption wavelength at 403 nm, which proved nano silver formation. The FTIR confirmed the carboxyl group in melanin to reduce the Ag^+ reduction as AgNPs, which promoted melanin covered in nano-silver surface. The SEM analysis showed that the morphology of Mel-AgNPs showed a spherical, and the particle diameter was about 30 nm. The element silver in the synthesized Mel-AgNPs was confirmed using EDX to exist silver in the synthetic Mel-AgNPS, and the crystal structure was characterized by XRD. The antibacterial activity experiments showed that Mel-AgNPs composites had inhibitory effect both on *Escherichia coli* and *Staphylococcus aureus*, and the inhibitory effects on *E.coli* is greater than *Staphylococcus*. In vitro antioxidant experiments showed that Mel-AgNPs composites had strong Fe^{3+} reduction ability and scavenging activity of DPPH and ABTS radical. The cytotoxicity experiments showed that Mel-AgNPs composite had weak toxicity to normal mouse fibroblast L929 and had inhibitory effect on human breast cancer cell line MCF-7, and Mel-AgNPs composites could down-regulate the level of BCl-2 gene in MCF-7 cells. This indicated that the material could inhibit the growth of cancer cells by regulating the pathways involved in the process of apoptosis and had certain anti-tumor activity. The anti-tumor experiments showed that Mel-AgNPs composites have strong antiviral capabilities to the H_3N_2 of the influenza virus, which can be used as a promising potential antiviral agent.

1. Introduction

In recent years, with the rapid development of nanotechnology, the application of nanomaterials is increasingly wide. Precious metal nanomaterials as an important branch of nanomaterials, including gold (AU), silver (Ag), copper (Cu), etc. Because of their unique physical and chemical properties, they have important application value in electronics, optical, biological and medicine, etc. [1–4]. Nano Silver (AgNPs) is an efficient and safe inorganic nano antibacterial agent, not only has strong antibacterial activity and low production cost, but also has advantages over other nano-materials in anti-virus, anti-cancer and other biomedical applications [5, 6]. However, the traditional method of preparing AgNPs has some defects, such as complex operation, high energy consumption and so on. And the larger surface of AgNPs make them extremely unstable in the process of dispersion, which is easy to agglomerate and affect their antibacterial properties. In addition, AgNPs also show certain cytotoxicity [7]. Therefore, the preparation of AgNPs with high stability and low cytotoxicity has become one of the key factors for their application.

Compared with the traditional physical and chemical methods, the biosynthesis of AgNPs has gradually become a research hotspot in recent years because of its simple operation, safety and environmental

protection. Currently, various biopolymers and biomolecules, such as gelatin [8], curcumin [9], chitosan [10], lignin [11] and plant extracts [12], have been used to synthesize AgNPs. Melanin as a kind of natural biological pigment, is a heterogeneous high molecular compound formed by oxidative polymerization of indole or phenolic compounds in nature. It is the most abundant and most extensive kind of amorphous pigment in biological pigments [13]. Natural melanin has excellent physical and chemical properties and a variety of biological functions, such as antioxidation, antibacterial activity, anti-tumor, etc., and has been widely used in the preparation of composites [14–16].

Therefore, in line with the concept of “green chemistry”, combining melanin with silver nanoparticles can not only reduce the cytotoxicity of AgNPs, but also improve their stability by complexing rich functional groups on the surface of melanin with silver ions. At the same time, it can also give full play to the antibacterial activity of silver nanoparticles and the antioxidant and anti-tumor activities of melanin. In order to develop a new type of functional nanomaterials with both biological activity and nano-material properties. In this paper, AgNPs were prepared using black sesame melanin as reducing agent and coating agent, and their antibacterial activity, antioxidation, anticancer and antiviral activity are studied.

2. Results And Discussion

2.1 Characteristic results of Mel-AgNPs

2.1.1 Ultraviolet-visible absorption spectra

In this study, black sesame melanin has the maximum absorption wavelength at 210 nm, and its absorbance value decreases with the increase of wavelength. This is consistent with the typical absorption characteristics of natural melanin in the UV-visible region. Mel-AgNPs exhibits a strong UV absorption spectrum at 403 nm due to its surface plasmon resonance (SPR) (Fig. 1A). It was observed with the naked eye that the color of the solution changed from colorless to light yellow and finally to yellowish brown, which confirmed the formation of Mel-AgNPs. This study is consistent with the results of Roy et al. [20].

2.1.2 Infrared spectrum

The results of FTIR analysis of melanin and Mel-AgNPs are shown in Fig. 1B.First, the absorption peak at 3423 cm^{-1} is attributed to the existence of hydroxyl (-OH) and amino ($-NH_2$) functional groups. Second, the absorption peak at 2850 cm^{-1} is attributed to the stretching vibration of C-H in aliphatic saturated alkane structure.Third, the absorption peak at 1645 cm^{-1} is caused by the stretching of aromatic C = C bond and carbon oxygen stretching vibration. Forth, the absorption peak at 1388 cm^{-1} is caused by the -OH deformation of phenolic hydroxyl groups. Then, the Crane O stretching and the symmetrical stretching of COO^- groups. And the absorption peaks at 1105 cm^{-1} and 997 cm^{-1} are attributed to the bending vibration of the C-H bond on the benzene ring. After the formation of Mel-AgNPs composites, some peaks of melanin shifted. The aromatic C = C bond in melanin and the peak position of carbon-oxygen in Mel-

AgNPs shift to 1816 cm^{-1}, which indicates that the carbonyl group in melanin reduces Ag^{+} to the absorption peak at 1388 cm^{-1} in AgNPs. As for melanin, so we can speculate that silver interacts with the indole ring of melanin. Our results are consistent with another study, which reported that chitosan interacts with metal salts and mediates the reduction process through its functional groups [21]

2.1.3 SEM electron microscope and energy dispersive X-ray (EDX) analysis

The SEM electron microscope images showed that the morphology of Mel-AgNPs was spherical, the size was relatively uniform, the particle size was about 30 nm. What is more, the dispersion was good, and there was no agglomeration (Fig. 1C). The EDX pattern was used to characterize the elemental composition of the synthesized Mel-AgNPs, which showed a characteristic absorption peak at 3 kev. This is the energy identification peak of silver, indicating that there is silver in Mel-AgNPs composites (Fig. 1D). The existence of C and O elements is caused by the coating of melanin on the nano-silver surface.

2.1.4 Dynamic light scattering (DLS) spectrum analysis

The average water and particle diameter of Mel-AgNPs measured by DLS were about 138 nm, a narrow distribution range, and a polydispersion coefficient (PDI) was 0.317, indicating that Mel-AgNPs can be dispersed in aqueous solution (Fig. 2A). The negative charge of Mel-AgNPs composite measured by Zeta potential is -42.05 ± 0.7 mV, and its electronegativity was mainly provided by the biomolecule melanin coated on the surface of AgNPs (Table 2). It was generally believed that the higher the absolute value of Zeta potential, the better the stability of the system. The absolute value of Zeta potential of the synthesized Mel-AgNPs composite was higher than that of 30 mV, indicating that it could remain stable in aqueous solution without precipitation.

2.1.5 X-ray diffraction (XRD) pattern analysis

The XRD patterns showed that Mel-AgNPs exists in the form of nanocrystals. The Bragg reflection peak 2θ showed four diffraction peaks at 37.9, 44.4, 64.15 and 77.3, corresponding to t (111), (200), (220) and (311) of silver nanocrystals, respectively. The results indicated that the structure of the prepared Mel-AgNPs composite was a typical face-centered cubic structure (Fig. 2B). Based on the XRD pattern, the grain size of the nanoparticles was determined by selecting the crystal plane, and the grain size of Mel-AgNPs was calculated to be about 39 nm by Scherrer equation. This is consistent with the results of SEM.

2.1.6 Thermogravimetric (TGA) atlas analysis

The TGA patterns of melanin and Mel-AgNPs showed that the single melanin began to lose weight at about 200°C and the weight loss rate reached 50% at about 310°C; but the prepared Mel-AgNPs composites showed good thermal stability, and the weight loss rate was less than 20% until 800°C (Fig. 2C), which also showed that the Mel-AgNPs composites had good thermal stability.

2.2 Determination of Mel-AgNP antibacterial activity

2.2.1 Determination by Agar diffusion method

Figure 3A showed the bactericidal photos of the diffusion of the bacteriostatic tablets, and Table S1 listed the results of the diameter of the bacteriostatic zone. It can be seen from Fig. 3A and Table S1 that melanin has no bacteriostatic zone on *E.coli* and *S.aureus*, while silver nitrate and Mel-AgNPs solution can produce bacteriostatic zone on *E.coli* and *S.aureus*, indicating that the antibacterial components of Mel-AgNPs mainly come from silver nanoparticles. And the bacteriostatic zone of Mel-AgNPs solution on *E.coli* and *S.aureus* is larger, indicating that the antibacterial effect of silver nanoparticles is better than that of silver ions. The diameter of bacteriostatic zone of Mel-AgNPs solution on *E.coli* and *S.aureus* was 12.0 ± 0.82 mm and 10.6 ± 0.75 mm, respectively, this showed that Mel-AgNPs solution had moderate inhibitory effect on *E.coli* and *S.aureus*. Last, the inhibitory effect on *E.coli* was better than that on *S.aureus*.

2.2.2 Determination of minimal inhibitory concentration (MIC) and minimum bactericidal concentration (MBC)

By diluting the coated plate *E.coli* and *S.aureus*, it was concluded that the suitable concentration of bacterial solution for MIC and MBC experiment is 10^{-3} CFU/mL. The MIC values of Mel-AgNPs composites to *E.coli* and *S.aureus* were shown in Fig. 3B and Table S2. When the concentration reached 0.1 mg/mL, the solution in the test tube was clarified, so the MIC of Mel-AgNPs composite to *E.coli* was 0.1 mg/mL. Similarly, when the concentration reached 0.15 mg/mL, the solution in the test tube was clarified, so the MIC of Mel-AgNPs composite to *S.aureus* was 0.15 mg/mL. The MBC values of Mel-AgNPs composites to *E.coli* and *S.aureus* were shown in Fig. 3C. When the concentration reached 0.2 mg/mL, there was no colony growth on the coated culture plate, indicating that the *E.coli* in the solution was completely killed, so the MBC of Mel-AgNPs composite to *E.coli* was 0.2 mg/mL. At the same time, when the concentration reached 0.3 mg/mL, there was no colony growth on the coated culture plate, indicating that the *S.aureus* in the solution was completely killed, so the MBC of Mel-AgNPs composite to *S.aureus* was 0.3 mg/mL.

2.2.3 Determination of bacterial growth curve

Figure 3D shows the growth inhibition curve of different concentrations of Mel-AgNPs composites on *E.coli* and *S.aureus*. As can be seen from the Fig. 3E, compared with the blank control group, the growth curves of *E.coli* and *S.aureus* treated with Mel-AgNPs composites changed significantly. And with the increase of the concentration of Mel-AgNPs composites, their growth trend was slower, which indicated that Mel-AgNPs composites can inhibit both *E.coli* and *S.aureus*. When the concentration increased to 0.1 mg/mL and 0.2 mg/mL, the OD_{600} value of *E.coli* almost did not increase, indicating that it had completely inhibited the growth of *E.coli*. When the concentration continued to increase to 0.2 mg/mL and 0.3 mg/mL, the OD_{600} value of *S.aureus* almost did not increase, indicating that it had completely inhibited the growth of *S.aureus*.

2.2.4 Observation of bacterial integrity by fluorescence imaging

The Propidium Iodide (PI) is a DNA binding dye which can penetrate damaged cell membranes to stain nuclei. Therefore, after the addition of the PI stain, the cells with red fluorescence observed under the fluorescence microscope were all apoptotic cells due to cell membrane rupture. Figure 3F is a fluorescence imaging after melanin-nano silver treatment *E.coli* and *S.aureus*. As can be seen from the figure, after Mel-AgNPs interacted with E.coli and S.aureus respectively, there was a significant red fluorescence in both groups of bacteria. However, the red fluorescence of the control group had fewer, indicating that Mel-AgNPs and *E.coli* and *S.aureus* can be directly in contact with these two bacteria, and quickly kill bacteria. And then, PI dye could enter the killed bacteria and dye them red.

In conclusion, the experimental results of antibacterial activity showed that the synthetic Mel-AgNPs composites have certain inhibitory effects on Gram-negative bacteria and Gram-negative bacteria, and the inhibition of *E.coil* was better than that on *S.aureus* inhibition. This indicated that the composite material had an high efficient and lasting antibacterial effect. The different antibacterial effects may be due to the different cell wall components of the two strains. *E. coli* is a Gram-negative bacteria with a thin cell wall (15–20 nm) and complex structure, which can be divided into outer membrane and peptidoglycan layer (2–3 nm). It is easy to be destroyed or even entered by antimicrobial agents. *S.aureus* belongs to Gram-positive bacteria, its cell wall is thicker (20–80 nm), with more than 20 layers of dense peptidoglycan, cell barrier function is stronger than *E. coli*, so the ability to resist antibacterial agents is stronger.

2.3 Determination of oxidation resistance of Mel-AgNPs composites in vitro

2.3.1 Determination of total antioxidant capacity

Figure 4A is the standard curve of FRAP determination with ferrous sulfate as the standard. The regression equation is Y = 1.247X + 0.110 and the correlation coefficient is R^2 = 0.997. Figure 4B shows the result of the total antioxidant capacity of Mel-AgNPs composites measured by FRAP. It can be seen from the diagram that the total antioxidant capacity of Mel-AgNPs composites has a dose-dependent relationship. And the FRAP value increases with the increase of the concentration of Mel-AgNPs composites, that is, the higher the concentration, the higher the FRAP value, the higher the content of reduced to Fe^{2+}-TPTZ in the reaction system. And there is a positive correlation between the sample concentration and the FRAP value. Therefore, Mel-AgNPs composites have strong Fe^{3+} reduction ability.

2.3.2 Determination of scavenging ability of DPPH free radicals

DPPH radical is a kind of paramagnetic compound with a single electron and a nitrogen center. When antioxidants are present, the DPPH radicals accept an electron or hydrogen atom to form a stable DPPH-H compound. As shown in Fig. 4C, Mel-AgNPs composites have certain scavenging activity on DPPH free radicals. When the concentration of Mel-AgNPs composites is 0.01 ~ 0.1 mg/mL, the scavenging ability is obviously enhanced, and the antioxidant activity is gradually enhanced. However, when the concentration continued to increase, the scavenging ability changed little, and the maximum scavenging rate of DPPH radical scavenging activity of Mel-AgNPs composites was 52%.

2.3.3 Determination of scavenging ability of ABTS free radicals

As shown in Fig. 4D, Mel-AgNPs composites have good scavenging activity on ABTS free radicals, and the antioxidant activity increases with the increase of the concentration of Mel-AgNPs composites. However, the scavenging ability of Mel-AgNPs composites to ABTS radical is slightly lower than that of ascorbic acid. As can be seen from the figure, the maximum scavenging rate of Vc is 99%. The maximum scavenging rate of ABTS radical scavenging activity of the composite material is 92%.

2.4 Determination of anti-tumor activity of Mel-AgNPs composites in vitro

2.4.1 Observation and determination of cell morphology

The growth state of the cells treated with the material can be preliminarily distinguished by observing the morphology of the cells. Fig. S1 shows the morphology of L929 cells treated with melanin, silver nitrate and different concentrations of Mel-AgNPs composite for 24 hours, in which (a) is the blank control group. It can be seen from the figure that the normal growth of L929 cells in the control group is adherent cells. The cells are long fusiform with a clear outline and uniform size. In addition, the cells fused closely, adhered to the wall, and grew in flakes at the bottom of the culture plate. At the same time, spherical mitotic cells were observed, which showed continuous proliferation and exuberant growth vitality. (b-f) were L929 cells were treated with low and medium concentrations of Mel-AgNPs composite for 24 hours. It can be seen from the Fig. S1 that the morphology of the cells was basically fusiform, which was consistent with the normal growth of L929 cells in the blank control group. The shape of the cells was obvious, the outline of the cells was very clear, the size is uniform, and the cells grew well. When L929 cells were treated with high concentration of Mel-AgNPs composite for 24 hours, the number of L929 cells decreased. However, the morphology is basically fusiform, and the cell morphology is obvious.

2.4.2 Cytotoxicity assay

The cytotoxicity of Mel-AgNPs composite to L929 cells and MCF-7 cancer cells was tested by MTT assay. It can be seen from the Fig. 5(a) that even if the concentration reached 0.2 mg/mL, the cell survival rate was still above 80%, and the cytotoxicity was grade 0. It was proved that Mel-AgNPs composite had no obvious cytotoxic effect on normal fibroblasts and had good biosafety effect. However, unlike normal

fibroblasts, Mel-AgNPs composites showed significant dose-inhibition dependence on MCF-7 cells. It can be seen from the Fig. 5(b) that as the concentration of Mel-AgNPs composites continued to increase, the inhibition rate of MCF-7 cells increased gradually. And when the concentration reached 0.4 mg/mL, the inhibition rate reached more than 70%, indicating that Mel-AgNPs composites can inhibit the proliferation of MCF-7 cells and have anti-tumor activity. According to the inhibition rate of different concentrations of Mel-AgNPs composite on MCF-7 cells, the semi-inhibition rate (IC_{50}) was calculated to be 0.285 mg/mL.

2.4.3 Effect of Mel-AgNPs composite on the expression of apoptotic genes

The RT-PCR was used to detect the expression of Bcl-2 gene in different concentrations of Mel-AgNPs composites. Bcl-2 gene is a proto-oncogene, which can inhibit apoptosis. As shown in Fig. 6, compared with the control group, Mel-AgNPs composite could significantly reduce the mRNA level of Bcl-2 gene in MCF-7 cells treated with Mel-AgNPs composite for 24 hours. With the increase of the concentration of Mel-AgNPs composite, the mRNA level of Bcl-2 gene decreased gradually in a significant dose-inhibition dependence, indicating that Mel-AgNPs composite could down-regulate the level of Bcl-2 gene in MCF-7 cells. And this also indicated that Mel-AgNPs composite could regulate the pathways involved in the process of apoptosis to prevent the growth of cancer cells.

2.5 Inhibitory effect of Mel-AgNPs Composites on Influenza virus H3N2

The cell survival rate was measured by MTT method. Using Reed-Muench method to calculate the following results: in the Mel-AgNPs treatment group, the $lgTCID_{50}$ of H_3N_2 virus on MDCK cells was 4.03/mL, the antiviral activity value of Mel-AgNPs was 2.48, and the antiviral activity rate was 99.67%.

3. Conclusion

In conclusion, this study used black sesame melanin as reducing agent and coating agent to successfully prepare Mel-AgNPs composites with uniform particle size and good dispersion. It's efficient, fast, green, and doesn't have any harmful by-products. The synthetic Mel-AgNPs exhibited excellent bioactivity in vitro, including antioxidant, antibacterial, anti-tumor and antiviral activities. Interestingly, the synthetic Mel-AgNPs composite material has good antibacterial and antiviral activity, which provides an idea for the development of new antiviral agents and the search for new virus control strategies. In addition, the synthetic Mel-AgNPs composite showed obvious selective killing ability against breast cancer cell line MCF-7, but there was no toxicity against normal mouse fibroblast cell line L929. Therefore, our findings confirm that biosynthetic Mel-AgNPs can be used as a promising anti-tumor agent with promising applications in the medical field.

4. Materials And Methods

4.1 Materials

Black sesame seed (*Nigella sativa* L.) was purchased from Shangqiu Gu Yu Liangyan Food Co., Ltd. Silver nitrate, sodium hydroxide, hydrochloric acid were purchased from National Pharmaceutical Group Chemical Reagent Co., Ltd. Cellulase, glucogenated enzyme, ascorbic acid, 1,1-diphenyl-2-picrylhydrazyl (DPPH), and 2,2´-azino-bis(3-ethylbenzothiazoline-6-sulfonic acid) diammonium salt (ABTS) were purchased from Solebo. MEM medium, 1640 medium, Green-streptomycin, Pancreatic enzyme, Fetal Bovine Serum, MTT, etc., purchased from Sigma Company, and other reagents were purchased from Tianjin Guangfu Science and Technology Development Co., Ltd.

4.2 Extraction and purification of black sesame black

The BSM was extracted from black sesame seed using a previously described method [16, 17]. Black sesame was ground into powder. Distilled water, cellulase and saccharifying enzyme were added to the precipitate, pH and temperature were adjusted to the optimal conditions for enzyme reaction 1h and then centrifugation. The crude extract was repeatedly dissolved by alkali and precipitated by acid, then washed with water and alcohol until neutral, and finally dried at 60℃ to obtain pure melanin.

4.3 Preparation of composite materials Mel-AgNPs

Silver nanoparticles were prepared by one-step method with silver nitrate as raw material and melanin as reducing agent and coating agent. Firstly, the melanin solution and $AgNO_3$ solution reacted with a volume ratio of 1:5 to avoid light for 50 min at 60℃. Then, the prepared samples were filtered by 0.22 μm nanofilm membrane, and the filtrate was collected to obtain Mel-AgNPs. Finally, the obtained solution was centrifuged at 10000 rpm for 15min, washed with distilled water, and then freeze-dried in vacuum at 4℃.

4.4 Characterization of composite materials Mel-AgNPs

4.4.1 Ultraviolet-visible absorption spectra (UV-vis) of Mel-AgNPs and its derivatives

The characteristic UV-vis spectra of Mel-AgNPs and its derivatives were analyzed in the wavelength range of 200–800 nm.

4.4.2 Fourier transform infrared spectroscopy (FTIR) analysis

A certain amount of Mel-AgNPs composite material and potassium bromide were mixed and crushed. The infrared spectrum could be obtained by scanning the infrared spectrum in the 4000 ~ 400cm^{-1} range with a single potassium bromide tablet as the background.

4.4.3 Scanning electron microscope (SEM) analysis

Using double-sided conductive adhesive, a small amount of Mel-AgNPs composites were placed on the sample table. After spraying gold, the morphology of Mel-AgNPs composite was observed under

scanning electron microscope.

4.4.4 Dynamic Light scattering Particle size Analyzer (DLS) analysis

The prepared Mel-AgNPs solution was diluted by a certain number of times, and placed in a dynamic light scattering particle size analyzer to measure the average particle size and Zeta potential.

4.4.5 X-ray diffraction (XRD) analysis

The crystallization properties of Mel-AgNPs composites were analyzed by X-ray diffraction.

4.4.6 Thermogravimetric (TGA) analysis

The thermal stability of BSM and Mel-AgNPs composites was analyzed by TGA.

4.5 Determination of Antibacterial activity of composite materials Mel-AgNPs

4.5.1 Agar diffusion method

Escherichia coli and *Staphylococcus aureus* were used as test bacteria. First of all, 100 μL bacterial suspension with a concentration of 1.0×10^6 CFU/mL was added to the surface of the solid medium and spread evenly with a coater. Then, the filter paper was soaked in samples for 2 hours, respectively. Thereafter, the soaking filter paper was affixed to the petri dish. Finally, the diameter of the bacteriostatic zone (mm) was observed and measured in the incubator at 37 ℃ for 24 hours, and the results were expressed by $X \pm s$.

4.5.2 Determination of minimal inhibitory concentration (MIC) and minimum bactericidal concentration (MBC)

The MIC and MBC of Mel-AgNPs against *E.coli* and *S.aureus* were measured by microdilution method. 4 mL LB medium and 100 μL samples (0.025, 0.075, 0.1, 0.15, 0.2, 0.25, 0.3 mg/mL) were used as experimental groups, PBS was added as blank group, shock culture,. After 24h, the MIC of melanin silver nanoparticles on such bacteria was obtained by observing the transparency of the medium in the test tube.. Next, 100 μL of the culture medium from all the clear and transparent test tubes was evenly coated on the solid medium and cultured at 37 ℃ for 24 hours. The corresponding concentration of the plate with less than 5 bacteria was the MBC of melanin-silver nanoparticles to this kind of bacteria.

4.5.3 Determination of bacteriostatic growth curve

20 μL bacterial suspension with concentration of 1.0×10^6 CFU/mL was inoculated in 96-well plate. Then, 200 μL LB liquid medium containing different concentrations of samples (0, 0.05, 0.05, 0.1 and 0.2 mg/mL) were added, 200 μL PBS was added to the control group. Finally, the 96-well plates were cultured at 37 ℃ and were taken out after 0, 2, 4, 6, 8, 10 and 12 hours, respectively, and their absorbance at 600

nm were determined. The growth curves of *E.coli* and *S.aureus* were drawn with culture time as abscissa and absorbance value as ordinate.

4.6 Determination of oxidation resistance of composites Mel-AgNPs in vitro

4.6.1 Determination of total antioxidant capacity

The total antioxidant capacity/iron reduction (FRAP) was determined according to the procedure previously described [17].

4.6.2 Determination of scavenging ability to DPPH radical

The removal activity of DPPH free radicals was measured according to the previously described method [18]. Sample solutions (2 mL) blended with DPPH solution (2 mL, DPPH concentration 25 mg/L in ethanol) and kept dark for 30 min at room temperature. The solution absorbance was measured at 510 nm. The activity of scavenging DPPH radicals was calculated as follows:

Scavenging activity(%)=[1-(A_1-A_2)/ A_0] × 100% (1)

where, A_0 represented the distilled water absorbance as a control sample, A_1 represented the tested sample absorbance, and A_2 represented the absorbance of sample solution itself.

4.6.3 Determination of scavenging ability to ABTS radical

The method for determining the scavenging ability of ABTS free radicals was based on the previously described method [19]. Blending the sample solution (1 mL) of different concentration with ABTS (3.0 mL, concentration 7 mmol/L) at room temperature for 30 min. Then, the solution absorbance was measured at 734 nm. The activity of scavenging ABTS radicals was calculated as follows :

Scavenging activity(%)=[1-(A_1-A_2)/ A_0] × 100% (2)

where, A_0 represented the distilled water absorbance as a control sample, A_1 represented the tested sample absorbance, and A_2 represented the absorbance of sample solution itself.

4.7 Anti-tumor activity of composites Mel-AgNPs in vitro

4.7.1 Cell culture

Mouse fibroblasts (L929 cells) and human breast cancer cells (MCF-7 cells) were purchased from the cell bank of the typical Culture Preservation Committee of the Chinese Academy of Sciences. The cells were cultured under standard conditions and incubated in an incubator with 37 ℃, 5% CO_2 and 95% humidity.

4.7.2 Cytotoxicity assay

The cytotoxicity of Mel-AgNPs was determined by MTT (3-(4-dimethylthiazolyl-2-yl)-2-diphenyl tetrazolium bromide) assay. L929 cells or MCF-7 cells were inoculated in 96-well plates at a density of 0.5 × 10^4 cells per well for 24 hours. Then the cells were incubated with samples (0.025, 0.05, 0.1, 0.15, 0.2, 0.25 and 0.3mg/mL) for 24 hours. Next, the medium was removed, 20 μL MTT (5 mg/mL) and 180 μL new medium were added and incubated for 4 h. Furthermore, the supernatant was removed, 200 μL DMSO was added, and the absorbance at 490 nm was measured. The survival rate and inhibition rate of cells in the presence of different concentrations of Mel-AgNPs were calculated according to formula (3). The untreated cells were used as the control group (Ar), and only the zeroing holes of the culture medium were added as the blank group (A_0).

The survival rate=(As-A_0/Ar-A_0)×100% (3)

4.7.3 Real-time quantitative PCR of apoptotic genes

In order to further evaluate the cytotoxicity of Mel-AgNPs composites, the real-time fluorescence quantitative PCR was used to detect the expression of Bcl-2 apoptosis-related genes in MCF-7 cells treated with Mel-AgNPs composites. The total RNA was extracted by Trizol method (including untreated and untreated MCF-7 cells). The cDNA was synthesized by HiFiScriptcDNASynthesisKit. Using cDNA as template, PCR amplification was carried out with FastSYBRMixture kit. The semi-quantitative RT-PCR amplification cycle program: pre-denaturation at 95 ℃ for 20s, denaturation at 95 ℃ for 3s and annealing at 60 ℃ for 30s, a total of 40 cycles. The GADPH was used as the internal reference gene for internal reference quantification, and the relative expression of Bcl-2 gene was calculated by $2^{-\triangle\triangle Ct}$ method. Table 1 lists the forward and reverse primer sequences of GADPH and Bcl-2 genes.

4.8 Antiviral activity of composites Mel-AgNPs in vitro

The MDCK cells of canine kidney cells were inoculated in 96-well plates at a density of 0.5×10^4 cells per well for 24 h. The Influenza A virus H_3N_2 was diluted with DMEM cell maintenance solution at a concentration gradient of 10 times, and 100 μL per well was added to 96-well plates respectively. At the same time, the control group was set up. The supernatant was discarded after incubation at 37℃ for 2 h, and washed with PBS for 3 times, and then added to the cell maintenance solution to continue culture for 1 week. The cytopathic changes (CPE) were observed under inverted microscope every day, and the logarithmic lgTCID50 of virus titer was calculated by Reed-Muench formula (4). The experiment was repeated 3 times.

$lgTCID_{50}$ = Distance ratio × The difference between the logarithm of the dilution + Logarithm of dilution above 50% lesion rate (4)

The neutralizing effects of Mel-AgNPs composites in RSV: the MDCK cells dog renal cell were cultured at 24-well plates and cultured at 37℃ for 24 h. The Mel-AgNPs composite material was mixed with an equal amount of H_3N_2 virus liquid and incubated at 4℃ for 1 h. Then the mixture was co-incubated with MDCK cells in the 24-well plate at 37℃ for 2 h, and the supernatant was discarded and washed once with PBS. Next, 1 mL of cell maintenance fluid was added. After 48–72 h, the viral control group had a

significant cytopathy, abandoned the culture solution, and PBS wash it once. Add 200 μL PBS to each well, freeze and thaw repeatedly at -80°C for three times. The 200 μL PBS per well was added repeatedly three times. The viruses released by cell lysis were collected and centrifuged at 3000rpm for 10min at 4°C to remove the cell debris. Finally, the supernatant virus samples were collected for virulence determination.

Declarations

Acknowledgments

All authors and co-authors are required to disclose any potential conflict(s) of interest when submitting an article (e.g. employment, consulting fees, research contracts, honoraria, advisory affiliations, etc.). This information should be included in an acknowledgments section at the end of the manuscript (before the references section). All sources of financial support for the project must also be disclosed in the acknowledgments section.

This research was supported by Research Project Supported by Shanxi Scholarship Council of China(2020-118), ShanXi key laboratory of pharmaceutical biotechnology, ShanXi Institute of biology(KF202002), Undergraduate Education and Teaching Reform project by North University of China (ZJ2020077), Innovation Project of Shanxi Graduate Education (2021Y599), the Key Research and Development Program of Shanxi Province (201803D221013-4, 201903D221033).

Data availability statement

The data used to support the findings of this study are available from the corre[1]sponding author upon request.

Conflict of interest

Authors state no conflict of interest.

References

1. Mansor M, Amir M, Julkapli N M. Gold hybrid nanomaterials: Prospective on photocatalytic activities for wastewater treatment application. MATER CHEM PHYS, 2019; 241:122415.
2. Varaprasad K, M López, D Núez. Antibiotic copper oxide-curcumin nanomaterials for antibacterial applications. J MOL LIQ, 2019; 300:112353.
3. Sukri S, Shameli K, Isa E. Green Synthesis of Zinc Oxide-Based Nanomaterials for Photocatalytic Studies: A Mini Review. *IOP Conference Series: Materials Science and Engineering*, 2021; 1051(1):012083.
4. Roy S, Rhim J W. Carrageenan-based antimicrobial bionanocomposite films incorporated with ZnO nanoparticles stabilized by melanin. FOOD HYDROCOLLOID, 2019; 90:500–507.

5. Dung T T N, Nam V N, Nhan T T. Silver nanoparticles as potential antiviral agents against African swine fever virus. MATER RES EXPRESS, 2019; 6(12):1–11.
6. Sharma R K, Cwiklinski K, Aalinkeel R. Immunomodulatory activities of curcumin-stabilized silver nanoparticles: Efficacy as an antiretroviral therapeutic. IMMUNOL INVEST, 2017; 46(8):833–846.
7. Guo Z, Zeng G M, Cui K P, et al. Toxicity of environmental nanosilver: mechanism and assessment[J]. Environmental Chemistry Letters, 2019; 17:319–333.
8. Muthivhi R, Parani S, May B, et al. Green synthesis of gelatin-noble metal polymer nanocomposites for sensing of Hg^{2+} ions in aqueous media. Nano-Structures & Nano-Objects, 2018; 13:132–138.
9. Petrov P D, Yoncheva K, Gancheva V, et al. Multifunctional block copolymer nanocarriers for co-delivery of silver nanoparticles and curcumin: Synthesis and enhanced efficacy against tumor cells. EUR POLYM J, 2016; 81:24–33.
10. Vijayakumar S, Malaikozhundan B, Parthasarathy A, et al. Nano Biomedical Potential of Biopolymer Chitosan-Capped Silver Nanoparticles with Special Reference to Antibacterial, Antibiofilm, Anticoagulant and Wound Dressing Material. J CLUST SCI, 2019; 31(2).
11. Jaiswal L, Shankar S, Rhim J W. Lignin-mediated green synthesis of AgNPs in carrageenan matrix for wound dressing applications. INT J BIOL MACROMOL, 2020; 159:859–869.
12. Al-Nuairi A G, Mosa K A, Mohammad M G. Biosynthesis, Characterization, and Evaluation of the Cytotoxic Effects of Biologically Synthesized Silver Nanoparticles from Cyperus conglomeratus Root Extracts on Breast Cancer Cell Line MCF-7. BIOL TRACE ELEM RES, 2020; 194(2):560–569.
13. Song S, Li S, Su N. Structural characterization, molecular modification and hepatoprotective effect of melanin from Lachnum YM226 on acute alcohol-induced liver injury in mice. FOOD FUNCT, 2016; 7(8): 3617–3627.
14. Gurme S T, Aware C B, Surwase S N. Synthesis of Melanin Mediated Silver Nanoparticles from Aeromonas sp. SNS Using Response Surface Methodology: Characterization with the Biomedical Applications and Photocatalytic Degradation of Brilliant Green. J POLYM ENVIRON, 2019.
15. Chu M Q, Hai W X, Zhang Z Y. Melanin nanoparticles derived from a homology of medicine and food for sentinel lymph node mapping and photothermal in vivo cancer therapy. BIOMATERIALS, 2016; 91: 182–199.
16. Rageh M M, El-Gebaly R H. Antioxidant activities and effects on γ-ray-induced DNA damage in the mouse. MUTAT RES-GEN TOX EN, 2018; 828.
17. Katalinic V, Milos M, Kulisic T. Screening of 70 medicinal plant extracts for antioxidant capacity and total phenols. FOOD CHEM, 2006; 94(4):550–557.
18. Fang Z, Zhang Y, Lue Y. Phenolic compounds and antioxidant capacities of bayberry juices. FOOD CHEM, 2009; 113(4):884–888.
19. Wang X, Wu Q, Wu Y. Response surface optimized ultrasonic-assisted extraction of flavonoids from Sparganii rhizoma and evaluation of their in vitro antioxidant activitiess. MOLECULES, 2012; 17(6):6769–6783.

20. Gurme S T, Aware C B, Surwase S N. Synthesis of Melanin Mediated Silver Nanoparticles from Aeromonas sp. SNS Using Response Surface Methodology: Characterization with the Biomedical Applications and Photocatalytic Degradation of Brilliant Green. J POLYM ENVIRON, 2019; 27(11):2428–2438.
21. Priya K, Mv B, Bj A. Chitosan-mediated synthesis of biogenic silver nanoparticles (AgNPs), nanoparticle characterisation and in vitro assessment of anticancer activity in human hepatocellular carcinoma HepG2 cells. INT J BIOL MACROMOL, 2020; 149:844–852.

Tables

Table 1 Amplification primer sequence

Gene	The forward primer（5’-3’）	The reverse primer（5’-3’）
GADPH	CACTAGGCGCTCACTGTTC	CAATACGACCAAATCCGTTGAC
Bcl-2	GATAACGGAGGCTGGGATGC	TCACTTGTGGCCCAGATAGG

Table 2 Zeta potential measurement results of Mel-AgNPs

Run	Zeta Potential（mV）	Half Width（mV）	Data Retention
1	-43.28	4.28	50%
2	-40.88	4.46	100%
3	-41.98	4.47	75%

Figures

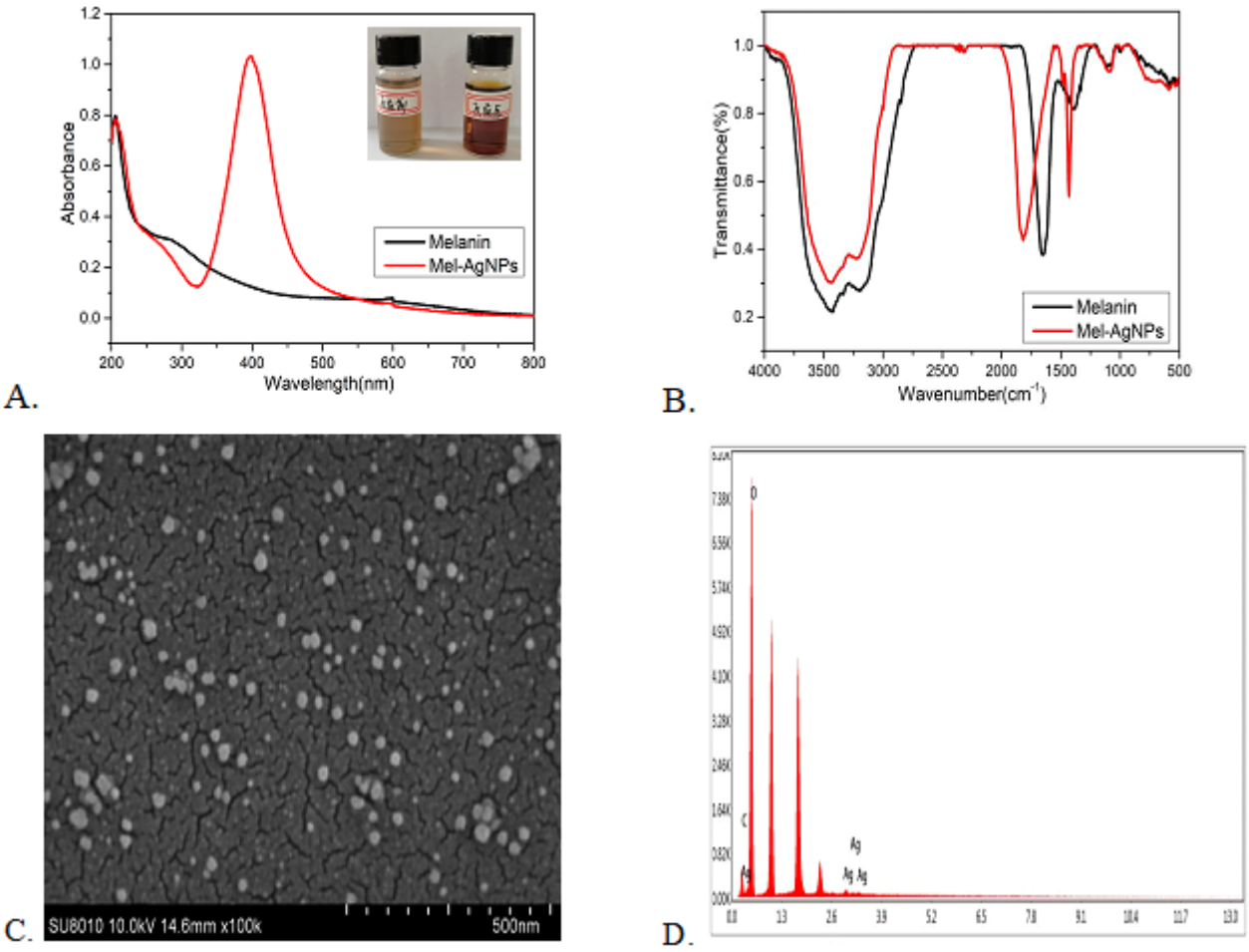

Figure 1

Characterization of Mel-AgNPs. (A) UV-Visible spectrum; (B) Infrared spectrum; (C) SEM image; (D) and EDX image of Mel-AgNPs.

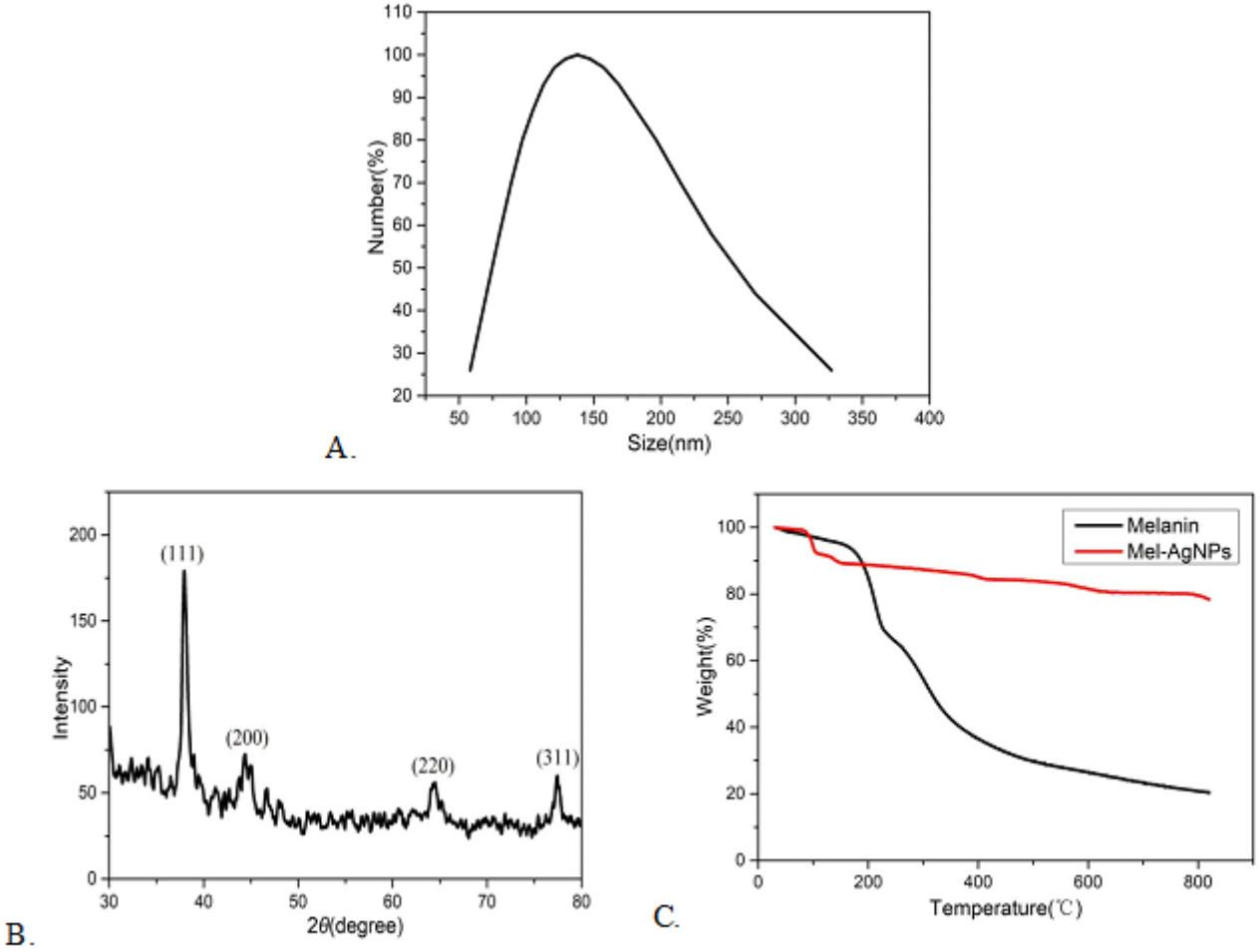

Figure 2

Characterization of Mel-AgNPs. (A) Particle size distribution; (B) XRD image; (C) and TGA image of Mel-AgNPs.

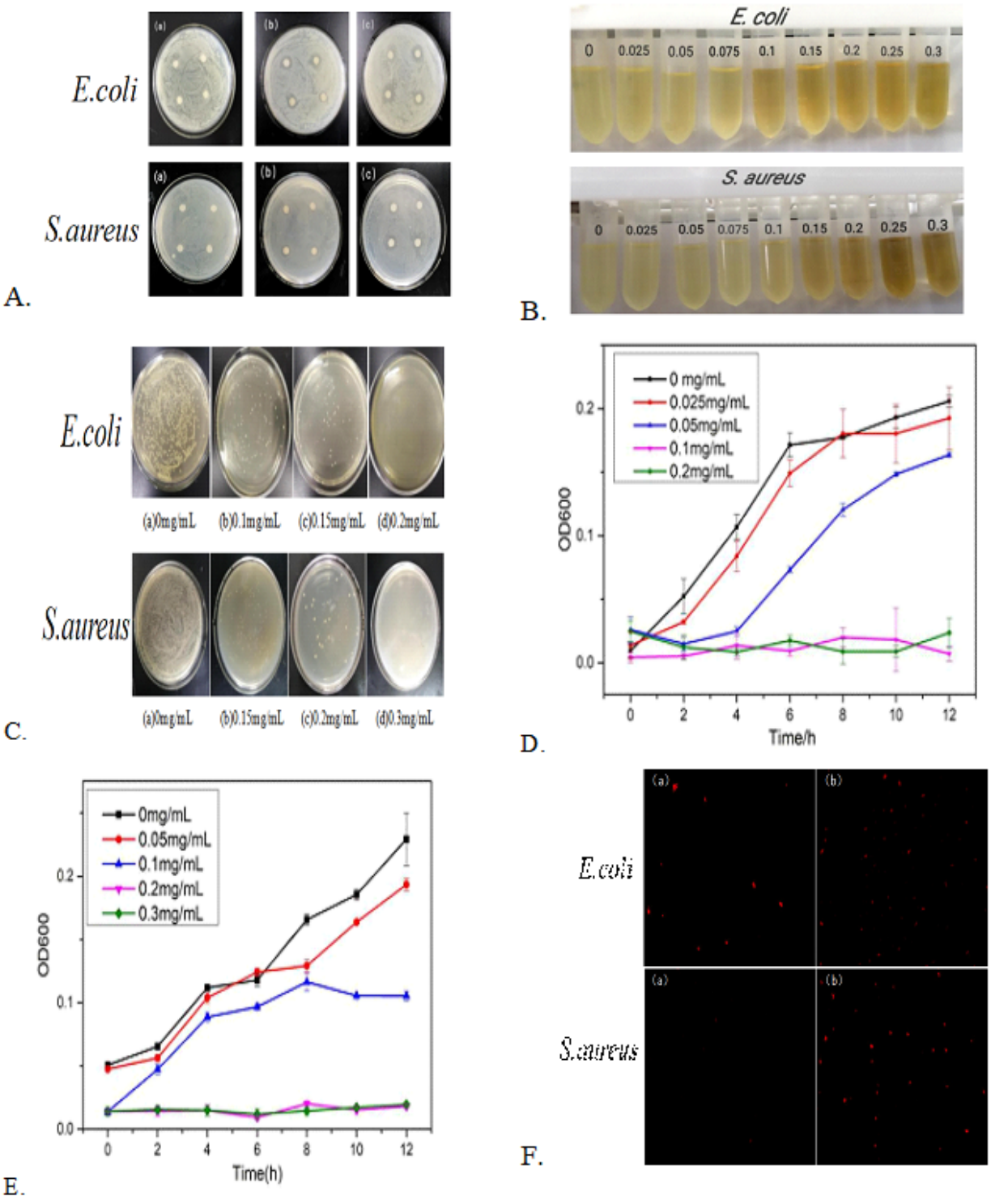

Figure 3

Determination of bacteriostatic properties. (A) Experimental results of inhibition zone of (a)Melanin, (b)$AgNO_3$, (c)Mel-AgNPs on E.coli and S.aureus; (B) Photo of MIC experiment results; (C) Sterilization results of different concentrations of Mel-AgNPs on E.coli and S.aureus; Growth inhibition curves of E. coli (D) and S. aureus (E) by different concentrations of Mel-AgNPs; (F) Fluorescence imaging of Mel-AgNPs treated with E.coli and S.aureus(a: control group, b: treatment group).

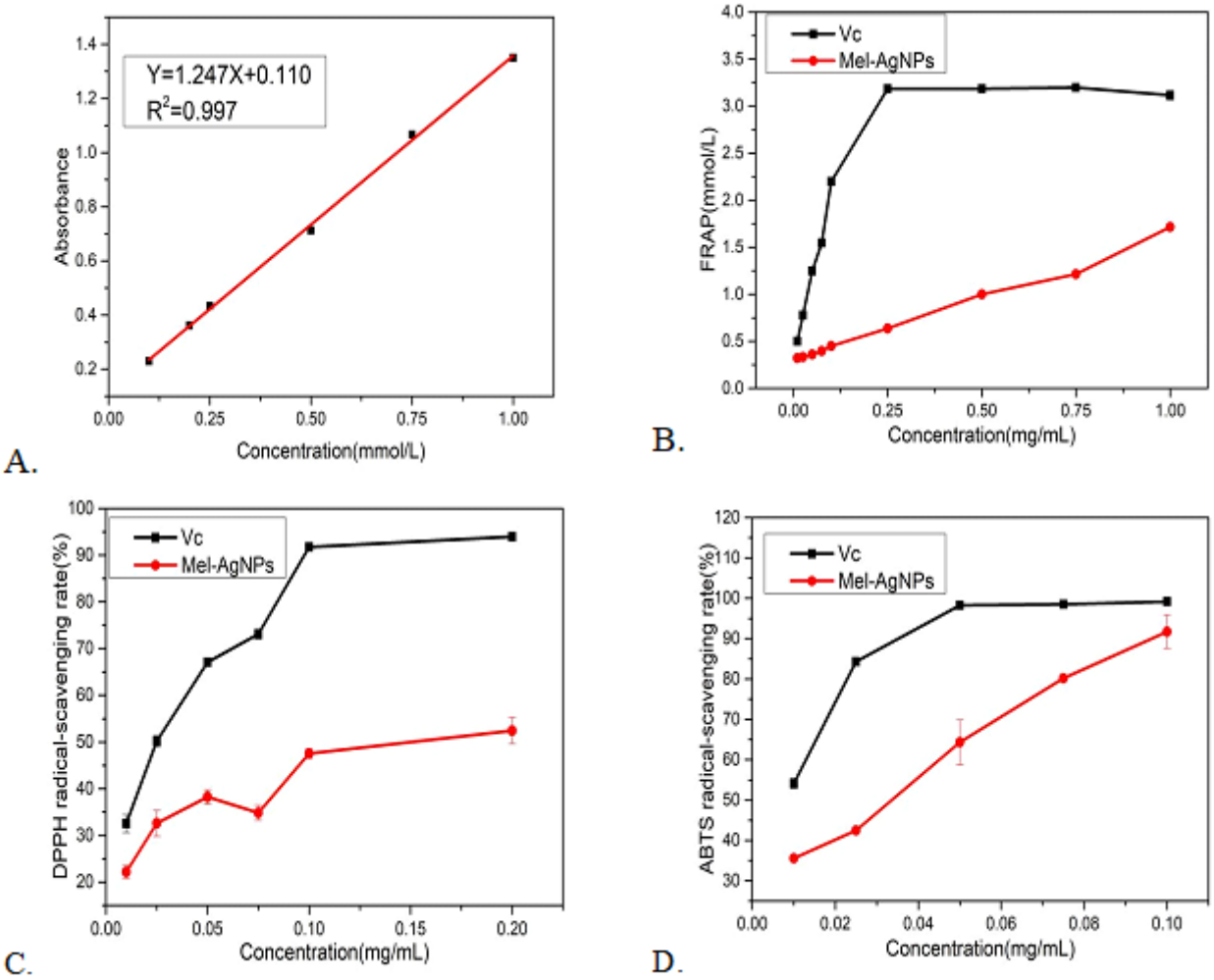

Figure 4

Determination of antioxidant activity. (A) Standard curve of ferrous sulfate; (B) Fe^{3+} reduction ability of Mel-AgNPs; (C) The ability of Mel-AgNPs to scavenging DPPH free radicals; (D) The ability of Mel-AgNPs to scavenging ABTS free radicals.

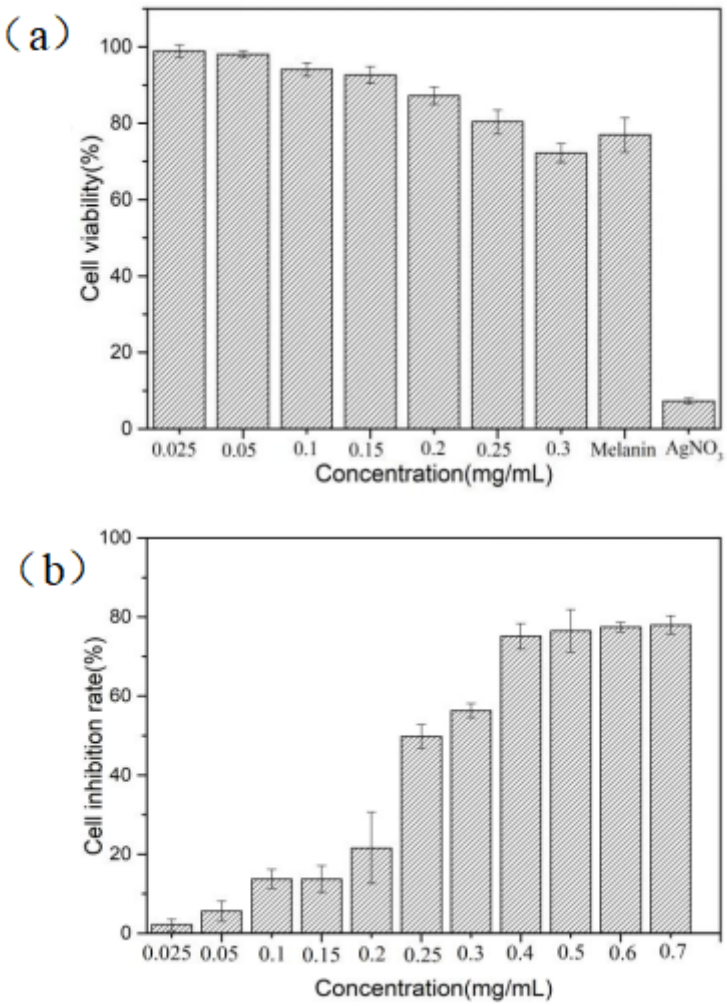

Figure 5

Cell viability of (a) L929 cell and (b) MCF-7 cells treated with different concentration of Mel-AgNPs.

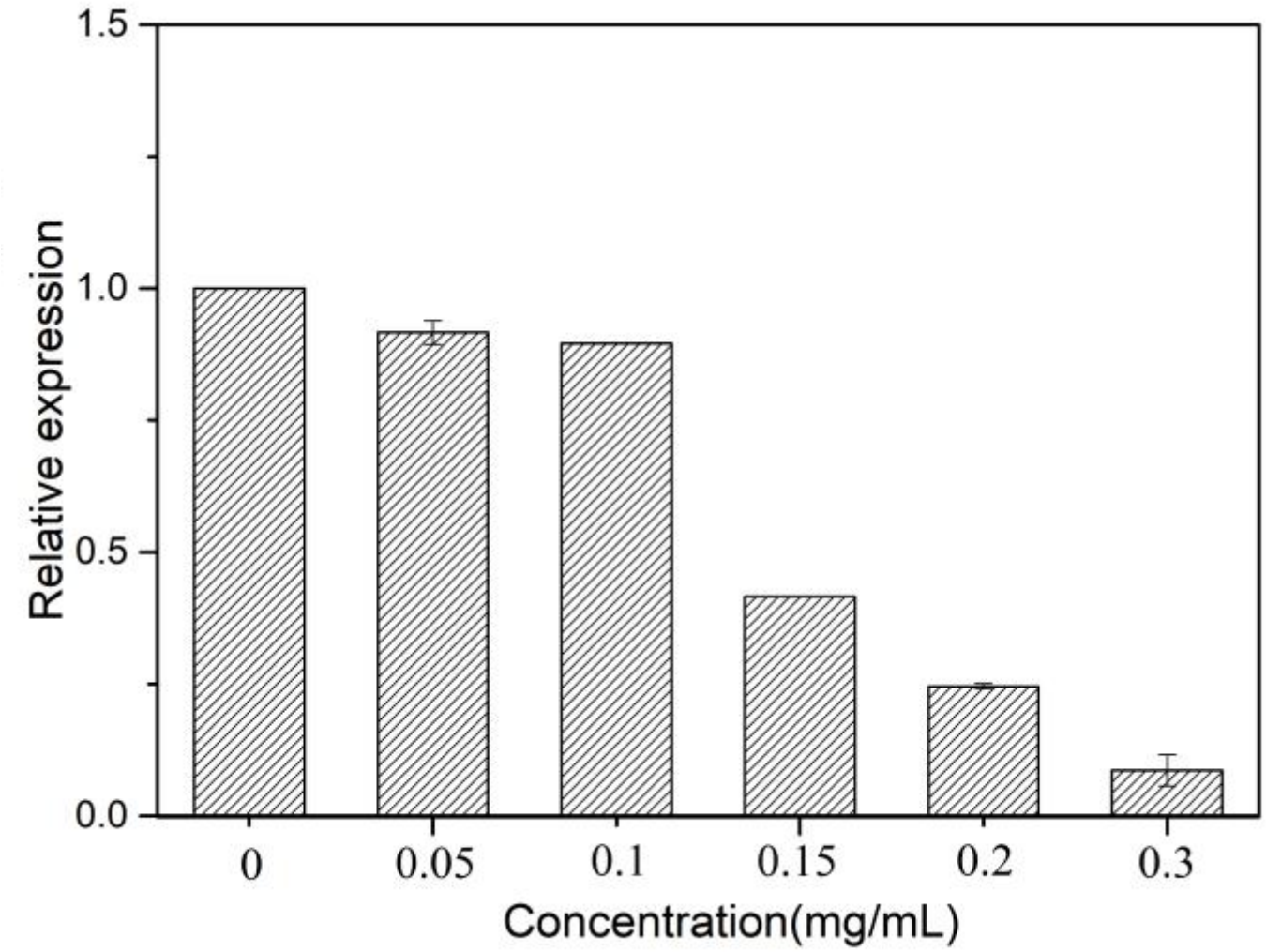

Figure 6

Different concentrations of melanin-nanosilver on the expression of Bcl-2 gene

Supplementary Files

This is a list of supplementary files associated with this preprint. Click to download.

- Supplementarymaterial.docx